

# RSC Advances



This is an *Accepted Manuscript*, which has been through the Royal Society of Chemistry peer review process and has been accepted for publication.

*Accepted Manuscripts* are published online shortly after acceptance, before technical editing, formatting and proof reading. Using this free service, authors can make their results available to the community, in citable form, before we publish the edited article. This *Accepted Manuscript* will be replaced by the edited, formatted and paginated article as soon as this is available.

You can find more information about *Accepted Manuscripts* in the [Information for Authors](#).

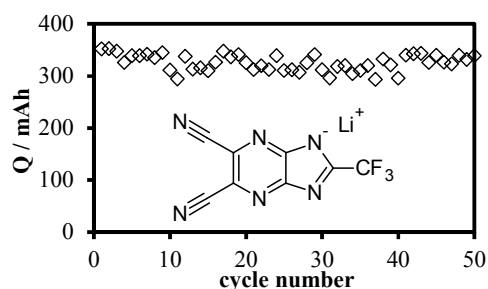
Please note that technical editing may introduce minor changes to the text and/or graphics, which may alter content. The journal's standard [Terms & Conditions](#) and the [Ethical guidelines](#) still apply. In no event shall the Royal Society of Chemistry be held responsible for any errors or omissions in this *Accepted Manuscript* or any consequences arising from the use of any information it contains.

# Imidazopyrazine-derived anion for lithium conducting electrolyte application

Leszek Niedzicki<sup>\*a</sup>, Jędrzej Korczak<sup>a</sup>, Anna Bitner<sup>a</sup>, Maria Bukowska<sup>a</sup>,

Przemysław Szczeciński<sup>a</sup>

## Table of content entry



Synthesized for the first time, LiTDPI salt in EC:DMC (1:2) tested as lithium conducting electrolyte shown high ionic conductivity, high lithium transference number and good cycling performance.

## Abstract

In this work we present new lithium salt of 4,5-dicyano-2-(trifluoromethyl)imidazopyrazine (LiTDPI) which is designed for use as electrolyte in lithium-ion cells. It was synthesized and completely characterized by NMR techniques. Salt is thermally stable up to 350°C and electrochemically stable in carbonate solvents up to +5.1 V vs. Li. Basic electrochemical characterization of this new lithium salt solutions show conductivity over 2 mS cm<sup>-1</sup> at room temperature and transference number higher than commercial reference salt, LiPF<sub>6</sub> (>0.4 in EC:DMC 1:2 ratio mixture). As a proof of concept, short cycling in a graphite half-cell shows good capacity (352 mAh g<sup>-1</sup>) and capacity retention

<sup>\*</sup> corresponding author, email: lniedzicki@ch.pw.edu.pl, phone: +48 22 234 7421, fax: +48 22 628 2741

<sup>a</sup> Warsaw University of Technology, Faculty of Chemistry, Department of Inorganic Chemistry and Solid State Technology, Noakowskiego 3, 00664 Warsaw, Poland

(96% after 50 cycles). Extremely good stability without compromising performance parameters show next leap in progress of tailoring efficient lithium-conducting electrolytes.

Keywords: lithium-ion; salt; electrolyte; synthesis; imidazopyrazine.

## 1. Introduction

For the last 20 years lithium batteries have been the fastest growing technology and now has established as the battery of choice in the energy storage market [1]. Such emerging, but soon-to-be mass applications of energy storage like electric vehicles and grid storage are focusing mainly on lithium-ion technology. All modern mobile devices, mobile phones and notebooks are basing solely on this technology as their energy source. Lithium-ion cells would not have their place on the market if not for the constant advance in their technology, *i.e.* development of component materials engineering and chemistry. However, while there is a plenty of scientific contributions on electrode materials structure and manufacturing, there is a huge gap in electrolytic materials for this type of cells. Apart from  $\text{LiPF}_6$ , no other salt has been used in wide scale production of commercial lithium-ion cells for the last 20 years. Although a lot of work and research on electrolytes is done every year, most works base on two-three salts, even though the salt influences most important cell parameters. For instance, its stability limits maximum cell voltage, conductivity influences maximum safe current density in constant discharge and lithium cation transference number influences charge-discharge cycle efficiency [2].

Despite the use of only two-three most popular salts among researchers, even those most popular ones, along with  $\text{LiPF}_6$ , have numerous disadvantages. To enumerate only the most important disadvantages:  $\text{LiPF}_6$  is a subject to hydrolysis, forming caustic HF and toxic  $\text{POF}_3$  [3,4] and has poor thermal stability [5];  $\text{LiClO}_4$  is potentially explosive in high

temperatures [6]; LiAsF<sub>6</sub> is toxic (as it contains arsenic); LiCF<sub>3</sub>SO<sub>3</sub> (LiTf) conducts poorly [7]; LiN(SO<sub>2</sub>CF<sub>3</sub>)<sub>2</sub> (LiTFSI) and LiN(SO<sub>2</sub>C<sub>2</sub>F<sub>5</sub>)<sub>2</sub> (LiBETI) corrode aluminum current collectors [8]; LiPF<sub>3</sub>(C<sub>2</sub>F<sub>5</sub>)<sub>3</sub> (LIFAP) is too expensive during production [4]; LiB(C<sub>2</sub>O<sub>4</sub>)<sub>2</sub> (LiBOB) forms high-resistance SEI at high concentrations [9]. Thus, there is still need for new concepts in the field of lithium salts for lithium-conducting electrolytes. Inspired by the success of the lithium 4,5-dicyano-2-(trifluoromethyl)imidazolide (LiTDI) [10-12] we decided to follow the path of anion design towards another “tailored” anion for the potential lithium-ion cell application.

Following our previous work on the lithium 5,6-dicyano-2-(trifluoromethyl)benzimidazolide (LiTDBI) [13], in this paper we propose new anion structure. Our new concept is basing on the LiTDBI, a benzene-derived anion, which has been previously modeled by Sheers et al. [14], and tested by our group in electrolytes. Electrochemical parameters of the LiTDBI solutions passed minimal requirements for the cell electrolyte [15]: its conductivity is over 1 mS cm<sup>-1</sup> at room temperature, lithium cation transference number is over 0.3 (in fact ca. 0.5), it is soluble in organic carbonates, compatible with graphite anode, has electrochemical stability over 4 V vs Li (in fact over 4.6 V vs Li) and thermal stability over 100°C (in fact over 280°C). Despite that, it has not defeated parameters set by the state of the art salt, the LiPF<sub>6</sub>. That may stem from the hydrogen presence in the LiTDBI salt structure. Although the only hydrogens in the molecule are bonded to the aromatic carbons, they can still have its share of intermolecular interactions thanks to possibility of hydrogen bonds forming with solvent molecules. Thus, in this paper we show enhancement of the LiTDBI structure made through removal of hydrogen atoms from the anion. This was performed by substituting carbon atoms in the aromatic ring with nitrogen atoms. This way we omitted unnecessary steric obstacles and possible proton sources, as well as the potential hydrogen bonds occurrence by the small cost of slightly

higher polarization of ring inner bonds. As a result we obtained lithium salt of the 4,5-dicyano-2-(trifluoromethyl)imidazopyrazine (which we abbreviated to LiTDPI).

In this paper basic properties of the salt are reported. Apart from standard spectroscopic characterization, we also investigated salt's properties that influence electrolyte parameters, such as stability. Basic electrochemical parameters of this new salt solutions were also tested. Finally, only as the proof of concept, we also have cycled the newly obtained electrolyte in a half-cell to check its potential for further development and optimization.

## 2. Experimental

### 2.1. Experimental techniques

Nuclear magnetic resonance (NMR) spectra were recorded on Varian Gemini 500. Samples for NMR experiments were dissolved in deuterated dimethyl sulfoxide (DMSO-d<sub>6</sub>, 99.96 atom % D, Aldrich). <sup>1</sup>H and <sup>13</sup>C chemical shifts are reported relative to DMSO-d<sub>6</sub>.

Thermogravimetric Analysis (TGA) was carried out on TA Instruments Q50 thermogravimetric analyzer. The carrier gas was argon and a heating rate was equal to 10 K min<sup>-1</sup>.

All samples for measurements were assembled in the argon-filled drybox with moisture level below 1 ppm. Prior to the assembly, the salt was vacuum-dried for 48 hours at 120°C. Solvents - propylene carbonate (PC), ethylene carbonate (EC), dimethyl carbonate (DMC) - were anhydrous and used as provided by Sigma-Aldrich (water content <20 ppm for PC and DMC, <50 ppm for EC).

Linear sweep voltammetry (LSV), cyclic voltammetry (CV), transference number, ionic conductivity and half-cell cycling measurements were carried out on VMP3 multichannel potentiostat (Bio-Logic Science Instruments) with frequency response analyzer

option. All electrochemical experiments except for the conductivity measurements were performed at ambient temperature.

LSV and CV experiments were realized with the custom-made three electrode Swagelok-type cell, where reference and counter electrodes are in form of discs and working electrode was a wire. Electrodes and separators soaked with electrolyte were sandwiched between the stainless steel punches. Platinum working electrode was a platinum wire put between separators from the side tight access port.

In case of LSV measurements were carried out in three-electrode Li | electrolyte | Pt system (with lithium metal as reference electrode). LSV scan rate was  $10 \text{ mV s}^{-1}$ .

In case of CV measurements were carried out in the same cell as LSV and used three-electrode Li | electrolyte | Al system (with lithium metal as reference electrode). CV scan rate was  $0.1 \text{ mV s}^{-1}$ .

For ionic conductivity measurements electrochemical impedance spectroscopy (EIS) was employed and samples were thermostated in Haake D50 cryostat where the temperature was varied from  $-20^\circ\text{C}$  to  $40^\circ\text{C}$  in  $10^\circ\text{C}$  increments (with a precision of  $0.05^\circ\text{C}$ ), allowing an hour for stabilization.

Lithium cation transference number was determined using standard Bruce-Vincent-Evans method [16] using the following equation:  $T_+ = (I_s (\Delta V - I_0 R_0)) / (I_0 (\Delta V - I_s R_s))$ , where  $\Delta V$  is the polarization voltage equal to 20 mV;  $I_0$  and  $I_s$  are the initial and the steady-state current during said polarization, respectively;  $R_0$  and  $R_s$  are resistances of the solid electrolyte interface (SEI) immediately before and after the polarization, respectively. The Li | electrolyte | Li cells were used for transference number experiments. Electrochemical impedance spectroscopy (EIS) used to obtain  $R_0$  and  $R_s$  has been performed with 5 mV amplitude over the 500 kHz-100 mHz frequency range with 10 points per decade. At least

three samples have been measured for each electrolyte composition for more consistent data. Detailed description of this method can be found in other papers [17].

Charge-discharge half-cell cycling with graphite used the Li | electrolyte | graphite cell. Standard commercial single-coated graphite electrode from MTI-XTL was used in that experiment. Cut-off voltages were set to 0.1-2.6 V values. Current was chosen in such a way that both discharge and charge processes would take 5 hours (C/5 rate). Half-cell contained  $0.7 \text{ mol kg}^{-1}$  LiTDPI in EC:DMC (1:2 weight ratio) electrolyte composition.

Charge-discharge half-cell cycling with LiNMO ( $\text{LiNi}_{0.5}\text{Mn}_{1.5}\text{O}_4$ ) used the Li | electrolyte | graphite cell. Standard commercial LiNMO electrode from Sigma-Aldrich was used in that experiment. Cut-off voltages were set to 3.5-5.0 V values. Current was chosen in such a way that both discharge and charge processes would take 5 hours (C/5 rate). Half-cell contained  $0.7 \text{ mol kg}^{-1}$  LiTDPI in EC:DMC (1:2 weight ratio) electrolyte composition.

## 2.2. Synthesis of lithium 5,6-dicyano-2-(trifluoromethyl)imidazopyrazine

Synthesis scheme is presented in Figure 1.

16 g (0.1 mol) of 5,6-diamino-2,3-dicyanopyrazine (TCI Europe NV) was added to 350 ml of acetonitrile. Subsequently, 30.2 g (0.14 mol) of trifluoroacetic anhydride was added under argon atmosphere to the reaction mixture and such mixture was kept under reflux for 6 hours (reaction progress controlled by TLC). Upon vacuum evaporation to dry mass, residue was dissolved in water, activated charcoal was added and stirred together for 10 minutes. Activated carbon was removed by filtering and the product was recrystallized from water. 19.6 g of 5,6-dicyano-2-(trifluoromethyl)imidazopyrazine were obtained (75% yield).  $T_m$  240-241°C.

$^1\text{H NMR}$  (DMSO- $d_6$ ): 11.75 (s, 1H, NH).

$^{13}\text{C}$  NMR (DMSO- $d_6$ ): 157.65 (q,  $\underline{\text{C}}\text{-CF}_3$ ,  $J(\text{C},\text{F}) = 39.2$  Hz), 147.1 (s, 2C, C=C shared by both rings), 126.6 (s, 2C,  $\underline{\text{C}}\text{-CN}$ ), 119.1 (q,  $\underline{\text{C}}\text{F}_3$ ,  $J = 272.5$  Hz), 115.2 (s, 2C,  $\underline{\text{C}}\text{N}$ ).

$^{19}\text{F}$  NMR (DMSO- $d_6$ ): one peak (not calibrated).

9.8 g of 5,6-dicyano-2-(trifluoromethyl)imidazopyrazine was treated with 5.5 g of lithium carbonate (50% excess) suspension in water. Mixture was stirred for ca. 5 minutes. The precipitate was separated and the water solution was evaporated under vacuum to obtain dry mass. Residue was dissolved in anhydrous acetonitrile and the undissolved precipitate was removed. Acetonitrile was evaporated under vacuum and the resulting salt was dried under vacuum at 110°C for 24 hours. Lithium salt of 5,6-dicyano-2-(trifluoromethyl)imidazopyrazine was obtained as a result. Salt decomposes at 356°C.

$^{13}\text{C}$  NMR (DMSO- $d_6$ ): 164.8 (q,  $\underline{\text{C}}\text{-CF}_3$ ,  $J(\text{C},\text{F}) = 35.7$  Hz), 151.9 (s, 2C, C=C shared by both rings), 123.8 (s, 2C,  $\underline{\text{C}}\text{-CN}$ ), 120.8 (q,  $\underline{\text{C}}\text{F}_3$ ,  $J = 272.2$  Hz), 116.1 (s, 2C,  $\underline{\text{C}}\text{N}$ ).

$^{19}\text{F}$  NMR (DMSO- $d_6$ ): one peak (not calibrated).

### 3. Results and discussion

Thermal stability of the salt was tested by means of TGA (thermogravimetric analysis). Obtained results show (Figure 2) decomposition onset at 350°C, which is much higher temperature than for most common salt in the battery industry,  $\text{LiPF}_6$  [18]. It is also much more stable than its benzimidazole analog, the  $\text{LiTDBI}$  (272°C). Unlike  $\text{LiPF}_6$ , and similarly to other imidazole-derived lithium salts,  $\text{LiTDPI}$  is stable in water solutions and is not a subject to hydrolysis. It means easier handling and less restrictions in salt storage conditions.  $\text{LiPF}_6$  on the other hand is decomposing already upon a contact with trace moisture, not to mention form solutions in it [19].

Electrochemical stability of the salt is a key factor for electrolyte performance.  $\text{LiTDPI}$  was tested for its electrochemical stability by means of LSV. LSV plot of 0.1 mol  $\text{kg}^{-1}$

LiTDPI solution in PC is presented on Figure 3. LiTDPI salt clearly shows stability up to 5.1 V vs. Li. This is more than enough for all kinds of contemporary electrode materials and allows for application and use of the full potential of new electrode concepts.

Ionic conductivity of LiTDPI was tested first in PC - the model solvent for organic carbonates family. Wide concentration range of salt, within three orders of magnitude, allowed to see the impact of association on conductivity, seen as qualitative activation energy changes throughout the concentration range. On the other hand, wide temperature range of measurements shows the stability of the new salt. Figure 4 presents the results of ionic conductivity measurements for LiTDPI-PC solutions. The highest conductivity, 1.9 mS cm<sup>-1</sup> at room temperature has been measured for 0.5 mol kg<sup>-1</sup> concentration. Conductivity at 0.2 mol kg<sup>-1</sup> concentration is very similar and is equal to 1.8 mS cm<sup>-1</sup>. The highest concentration, 1 mol kg<sup>-1</sup>, which was also the maximum solubility of LiTDPI in PC, had much smaller conductivity, 1.4 mS cm<sup>-1</sup>. However, activation energy for the highest conductivity is clearly much higher than for lower concentrations. Thus, increase of the conductivity with the temperature is much higher. So while at -20°C 1 mol kg<sup>-1</sup> concentration starts from the same conductivity value as 0.1 mol kg<sup>-1</sup>, at 60°C it levels with the that of 0.2 mol kg<sup>-1</sup>, which is the second to 0.5 mol kg<sup>-1</sup> ionic conductivity. Lower concentrations are ordered with their concentration in conductivity terms with the exception of the lowest one, 0.001 mol kg<sup>-1</sup>, which has its conductivity slightly higher than that of 0.002 mol kg<sup>-1</sup> and it might be the result of early association effects. Clearly, different behavior of 1 mol kg<sup>-1</sup> concentration only might be a result of it being the highest concentration and maximum solubility, which effects typically with higher viscosity and advanced association. Higher activation energy is the proof of such argument.

Figure 5 shows the behavior of LiTDPI solutions in EC:DMC (1:2 weight ratio) mixture. It depicts ionic conductivity vs temperature plot. Due to a higher complexity of the

system (ternary), association is more complicated, so it is not surprising that conductivity dependence on concentration is more complicated than in simpler system (LiTDPI-PC). Although at the lowest concentrations dependence is similar to PC solutions, that is conductivity of 0.001 mol kg<sup>-1</sup> solution is higher than that of 0.002 mol kg<sup>-1</sup> solution and the ionic conductivity of increasing concentrations from 0.002 mol kg<sup>-1</sup> and on are monotonically rising. However, as soon as at 0.1 mol kg<sup>-1</sup> it starts to change, because 0.5 mol kg<sup>-1</sup> conductivity (1.13 mS cm<sup>-1</sup> at 20°C) is lower than that of 0.1 mol kg<sup>-1</sup> (1.16 mS cm<sup>-1</sup>). Above 0.5 mol kg<sup>-1</sup> there is a sudden jump of the conductivity – 2.94 mS cm<sup>-1</sup> at 0.7 mol kg<sup>-1</sup> and similar, but a little smaller one, at 1 mol kg<sup>-1</sup> – 2.84 mS cm<sup>-1</sup>. It is also plainly visible that activation energies of 0.7 and 1 mol kg<sup>-1</sup> solutions are much higher than that of lower concentration solutions. That last observation overlaps with the one made for results for PC solutions and strengthen arguments about the impact of association at such high concentrations.

Another very important parameter for electrolytes in order to assess their potential for real world application is lithium cation transference number. It does not only affects yield of charge-discharge cycle, but also is a component to lithium cation conductivity when multiplied by ionic conductivity. Lithium cation conductivity is a key factor for evaluation of the electrolyte, as it affects also rate capability of the final cell. In case of LiTDPI, solutions with concentrations which show high lithium cation transference number values overlaps with those of high ionic conductivity. In it, LiTDPI is similar to other weakly-coordinating imidazole-derived anions, and it is different from most of other, mostly inorganic, cations. The latter usually keep reciprocal dependency between lithium cation transference number and ionic conductivity. Figure 6 presents results of transference number measurements for LiTDPI solutions in both PC and in mixture of EC and DMC (1:2 weight ratio). Results for PC solutions are slightly better on average than ones for EC:DMC mixture, they are also more

stable throughout the concentration range with a notable exception of the highest concentration ( $1 \text{ mol kg}^{-1}$ ). Even though lithium cation transference numbers of EC:DMC solutions have decreased values for  $0.001\text{-}0.01 \text{ mol kg}^{-1}$  range, the most important results from the application point of view are relatively high and surpass the 0.4 value. It is also important, that they overlap with the highest conductivity, yielding lithium cation conductivity over  $1 \text{ mS cm}^{-1}$  (*e.g.* at  $1 \text{ mol kg}^{-1}$ ,  $2.84 \text{ mS cm}^{-1} \times 0.43 = 1.22 \text{ mS cm}^{-1}$ ). There is also a very high value of that parameter for  $1 \text{ mol kg}^{-1}$  solution of LiTDPI in PC, namely 0.55, which is also much above traditional, inorganic lithium salts.

Finally, to make the final proof that the LiTDPI salt is possible to apply as a lithium conducting electrolyte and has a potential for application in energy storage, preliminary half-cell cycling has been performed. Graphite |  $0.7 \text{ mol kg}^{-1}$  LiTDPI-EC:DMC (1:2) | Li half-cell was assembled and tested with charge-discharge cycling. Figure 7 shows the result of such cycling. It begins at quite a high capacity of  $351 \text{ mAh g}^{-1}$ , while the theoretical value of the capacity for graphite is  $372 \text{ mAh g}^{-1}$ . Thus, it is 94% of the theoretical value. Moreover, after 50 cycles the capacity retention is very good, as it keeps on the similar level until the 50<sup>th</sup> cycle, at which it is  $338 \text{ mAh g}^{-1}$ , so it is 96% of the initial capacity. That proves, that LiTDPI is compatible with the graphite anode and it is very stable as an electrolyte. Also, it is not decomposing at the high or low voltage applied to the cell during cycling.

Additional two preliminary measurements were made for the purpose of testing potential of LiTDPI to use in high-voltage cells. Firstly, the corrosiveness of  $0.7 \text{ mol kg}^{-1}$  LiTDPI in EC:DMC (1:2 weight ratio) against aluminum collector was tested. Result of this measurement is shown on Figure 8 in supplementary materials. Even though the CV rate was very slow ( $0.1 \text{ mV s}^{-1}$ ), there is no visible sign of corrosion until 4.6 V vs. Li and even then it is not abrupt (until 5.1 V vs. Li). Secondly, the same  $0.7 \text{ mol kg}^{-1}$  LiTDPI in EC:DMC (1:2 weight ratio) electrolyte was preliminarily tested with the high-voltage cathode in the

$\text{LiNi}_{0.5}\text{Mn}_{1.5}\text{O}_4$  |  $0.7 \text{ mol kg}^{-1}$  LiTDPI-EC:DMC (1:2) | Li half-cell. The result of the cycling is shown on the Figure 9. Although initial discharge capacity is quite good ( $80 \text{ mAh g}^{-1}$ ), it is decreasing steadily and fast. As the electrolyte was not optimized for these measurements and it is the only cathode material tested so far, it is possible, that LiTDPI is not compatible with this particular cathode. Also, formation of the cell should be optimized, which was not the case here. However, even that very preliminary test proves salt stability against high potentials in the cell, which was the main reason for this measurement.

The results obtained for LiTDPI solutions are very important, because they show that it is possible to tweak the structure of the anion of the salt in the way, that no property is getting worse and no parameter is getting lower. Although the difference between TDPI and TDBI anion (benzimidazole vs imidazopyrazine rings) is not very big, neither it is subtle. The change proposed here improve most of the parameters distinctively and consistently. Improvement takes place for both thermal and electrochemical stability (by almost  $80^\circ\text{C}$  and  $0.35 \text{ V}$ , respectively). This means that the ring has higher stability due to HOMO energy level change as a result of structural change. Also, ionic conductivity and lithium cation conductivity are also better, which can be explained by a weaker coordination of the lithium cation and higher mobility of the anion. Those are affecting transference numbers and association which leads to lithium cation conductivity. Weaker coordination, lower association level and stability improvement are the result of getting rid of hydrogen atoms. Hydrogen atoms are prone to form hydrogen bonds with the solvent (especially such as carbonates) and be a weakest link in terms of stability (radical formation). The other, beneficial properties of the structures are left, meaning symmetry, presence of electron withdrawing groups and the aromatic skeleton (so-called Hückel anions). Thus, the main thesis of the concept has been proven, that assumed improvement of the structure is in fact the improvement of practical features.

#### 4. Conclusions

In the present work, we have presented synthesis, characteristics and basic properties of solutions of a completely new lithium salt tailored for application as a lithium-ion conducting electrolyte. The aim was to obtain new weakly-coordinating anion that could provide better ionic transport than previous generations of lithium salts, while keeping good safety and easiness of handling properties. Synthesis of anion itself is one-step and easy in terms of handling the substrates and the product, as no special means, equipment or materials purity are needed for its effective synthesis. We also characterized new substance with basic spectra data as well as its thermal and electrochemical stabilities, which are very good comparing to the state-of-the-art ( $\text{LiPF}_6$ ), namely up to  $350^\circ\text{C}$  and  $5.1\text{ V vs Li}$ . Thus, it is much more stable than its other imidazole-derived predecessors, like LiTDI or even newest one, LiTDBI (another salt with two-ring aromatic anion). Basic tests also show good transport properties, with two-fold increase of conductivity comparing to LiTDBI, close to  $3\text{ mS cm}^{-1}$ , and similar lithium cation transference number, over 0.4. Overall, lithium cation conductivity (ionic conductivity multiplied by lithium cation transference number), as well as safety/stability of the new LiTDPI salt is better than LiTDBI, which is undoubtedly an advance. It is also proof of the possible achievements using Hückel-type weakly-coordinating anions. Finally, as a proof of concept, electrolyte containing LiTDPI were preliminary tested in half-cell with graphite anode, showing good compatibility and excellent capability retention over 50 cycles. There is also no difference in that good performance with electrode comparing to LiTDBI, which is another success of the new anion. All these LiTDPI benefits and lack of negative differences towards LiTDBI are confirming the initial assumption that removing hydrogens from the anion structure would be beneficial for the salt performance. Apart from achieving theoretical objectives, LiTDPI is also proving with its great half-cell

performance, that there is application potential for that salt and it deserves more interest in the future.

### Acknowledgements

This work was financially supported by Warsaw University of Technology.

The research leading to these results has received funding from the European Union Seventh Framework Programme (FP7/2007-2013) under grant agreement number 608502 (Project SIRBATT).

### References

- [1] Lux Research, Beyond Lithium-Ion: A Roadmap for Next-Generation Batteries, March 2013, LREVI-R-13-1.
- [2] M. Marcinek, J. Syzdek, M. Marczewski, M. Piszcz, L. Niedzicki, M. Kalita, A. Plewa-Marczewska, A. Bitner, P. Wieczorek, T. Trzeciak, M. Kasprzyk, P. Łęzak, Z. Zukowska, A. Zalewska, W. Wieczorek, *Solid State Ionics* 276 (2015) 107.
- [3] T. Kawamura, S. Okada, J.-I. Yamaki, *J. Power Sources* 156 (2006) 547.
- [4] H.-B. Han, S.-S. Zhou, D.-J. Zhang, S.-W. Feng, L.-F. Li, K. Liu, W.-F. Feng, J. Nie, H. Li, X.-J. Huang, M. Armand, Z.-B. Zhou, *J. Power Sources* 196 (2011) 3623.
- [5] X. Zhang, P.N. Ross, Jr., R. Kostecki, F. Kong, S. Sloop, J.B. Kerr, K. Striebel, E.J. Cairns, F. McLarnon, *J. Electrochem. Soc* 148 (2001) A463.
- [6] R. Jasinski, S. Carroll, *J. Electrochem. Soc.* 117 (1970) 218.
- [7] A. Webber, *J. Electrochem. Soc.* 138 (1991) 2586.
- [8] S.-T. Myung, M. Hitoshi, Y.-K. Sun, *J. Mater. Chem.* 21 (2011) 9891.
- [9] K. Xu, S. Zhang, T.R. Jow, *Electrochem. Solid-State Lett.* 8 (2005) A365.

- [10] L. Niedzicki, G.Z. Żukowska, M. Bukowska, P. Szczeciński, S. Grugeon, S. Laruelle, M. Armand, S. Panero, B. Scrosati, M. Marcinek, W. Wieczorek, *Electrochim. Acta* 55 (2010) 1450.
- [11] L. Niedzicki, S. Grugeon, S. Laruelle, P. Judeinstein, M. Bukowska, J. Prejzner, P. Szczeciński, W. Wieczorek, M. Armand, *J. Power Sources* 196 (2011) 8696.
- [12] D.W. McOwen, *Developing New Electrolytes for Advanced Li-ion Batteries*, [Ph.D. Thesis], North Carolina State University, Raleigh, North Carolina, 2014.
- [13] L. Niedzicki, P. Oledzki, A. Bitner, M. Bukowska, P. Szczecinski, submitted.
- [14] J. Scheers, P. Johansson, P. Szczecinski, W. Wieczorek, M. Armand, P. Jacobsson, *J. Power Sources* 195 (2010) 6081.
- [15] D. Linden, T.B. Reddy (Ed.), *Handbook of Batteries* (3rd Edition), McGraw-Hill 2002.
- [16] P.G. Bruce, C.A. Vincent, *J. Electroanal. Chem.* 225 (1987) 1.
- [17] L. Niedzicki, M. Kasprzyk, K. Kuziak, G.Z. Zukowska, M. Marcinek, W. Wieczorek, M. Armand, *J. Power Sources* 196 (2011) 1386.
- [18] X.-G. Teng, F.-Q. Li, P.-H. Ma, Q.-D. Ren, S.-Y. Li, *Thermochimica Acta* 436 (2005) 30.
- [19] A.V. Plakhotnyk, L. Ernst, R. Schmutzler, *J. Fluorine Chem.* 126 (2005) 27.

**Figure captions**

Fig. 1. Synthesis scheme for the lithium 5,6-dicyano-2-(trifluoromethyl)imidazopyrazine (LiTDPI) salt described in the text.

Fig. 2. Thermogravimetric analysis plot of the LiTDPI salt with the DTG plot.

Fig. 3. Linear sweep voltammetry of the  $\text{Li} \mid 0.1 \text{ mol kg}^{-1} \text{ LiTDPI-PC} \mid \text{Pt}$  system with a lithium metal as the reference electrode.

Fig. 4. Dependence of ionic conductivity on temperature for a wide range of the LiTDPI concentrations in a propylene carbonate.

Fig. 5. Dependence of ionic conductivity on temperature for wide range of the LiTDPI concentrations in a mixture of ethylene carbonate and dimethyl carbonate (1:2 weight ratio).

Fig. 6. Dependence of lithium cation transference number on the LiTDPI concentration in a propylene carbonate and in a mixture of ethylene carbonate and dimethyl carbonate (1:2 weight ratio).

Fig. 7. Discharge anodic capacities during cycling of the  $\text{graphite} \mid 0.7 \text{ mol kg}^{-1} \text{ LiTDPI-EC:DMC (1:2 weight ratio)} \mid \text{Li}$  half-cell at the C/5 rate.

Fig. 8. Cycling voltammetry of the  $\text{Li} \mid 0.7 \text{ mol kg}^{-1} \text{ LiTDPI-PC} \mid \text{Al}$  system with a lithium metal as the reference electrode.

Fig. 9. Discharge cathodic capacities during cycling of the  $\text{LiNMO (LiNi}_{0.5}\text{Mn}_{1.5}\text{O}_4) \mid 0.7 \text{ LiTDPI-EC:DMC (1:2 weight ratio)} \mid \text{Li}$  half-cell at the C/5 rate.

Fig. 1.

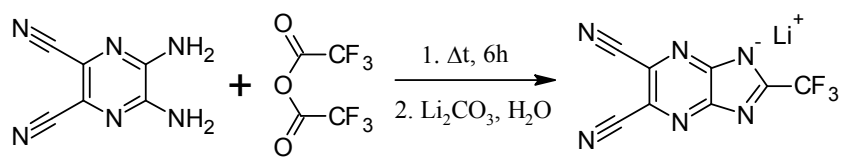


Fig. 2.

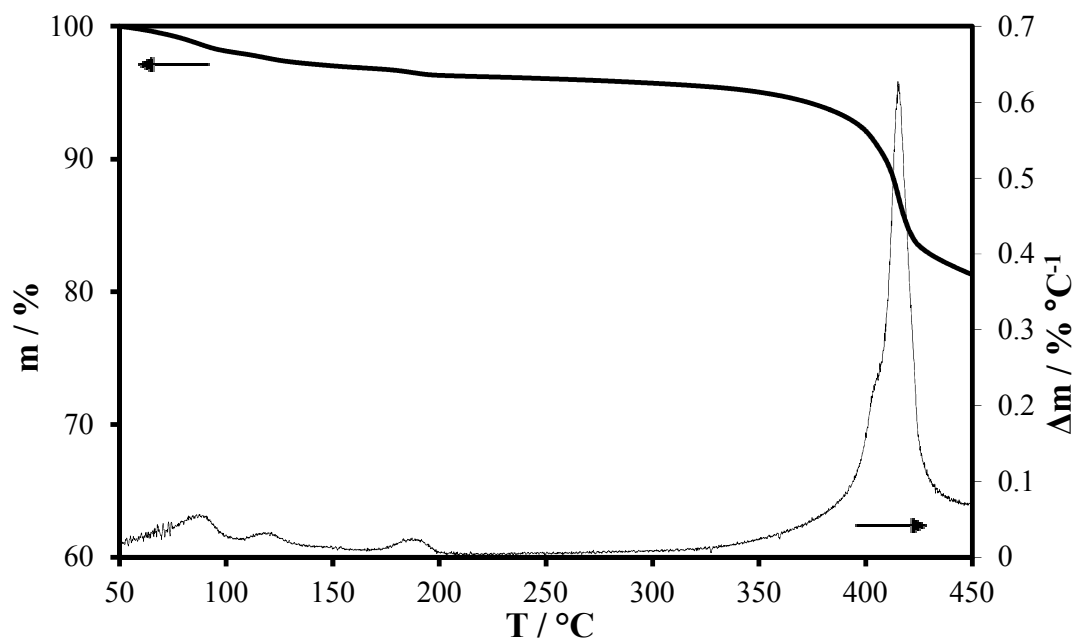


Fig. 3.

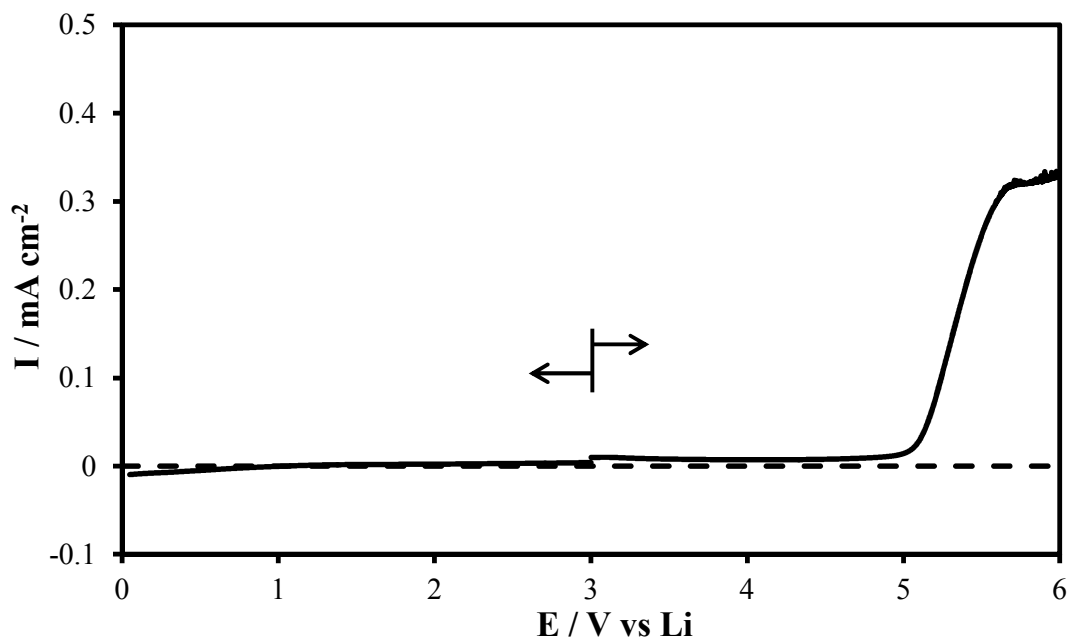


Fig. 4.

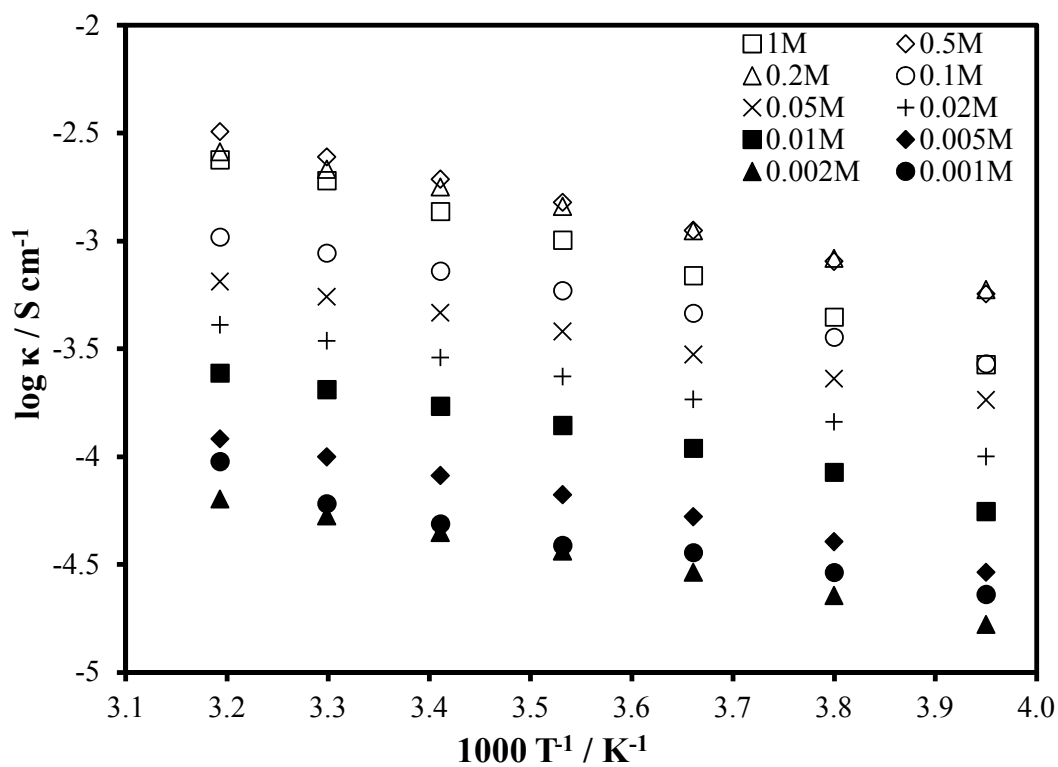


Fig. 5.

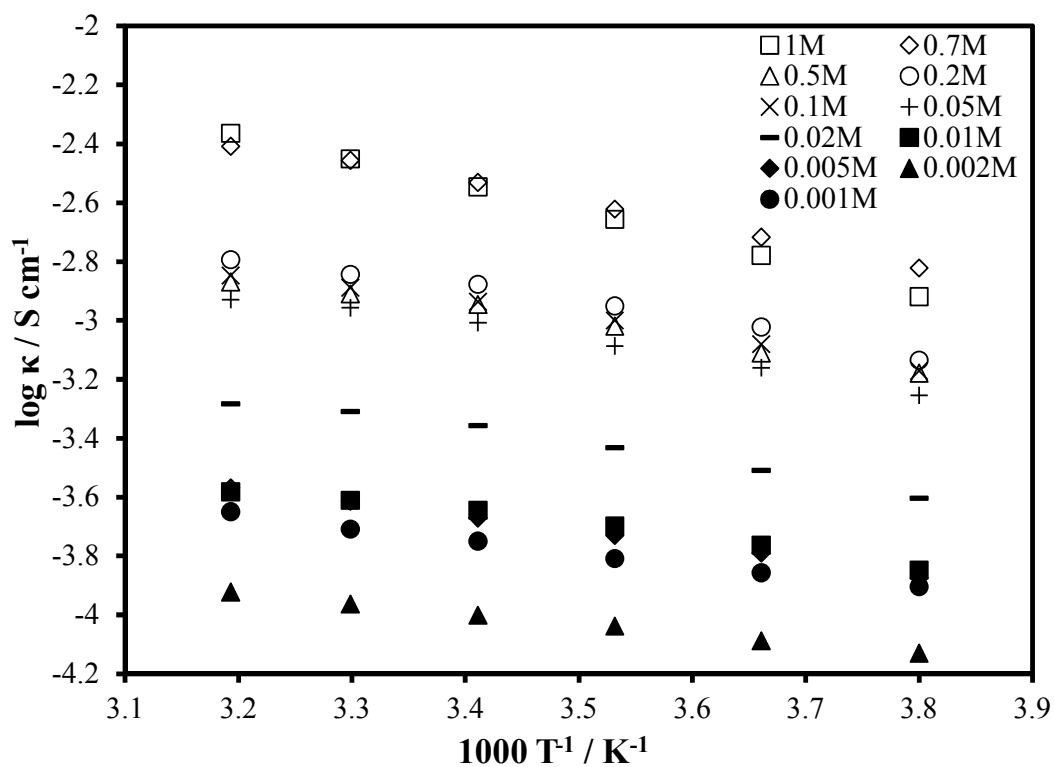


Fig. 6.

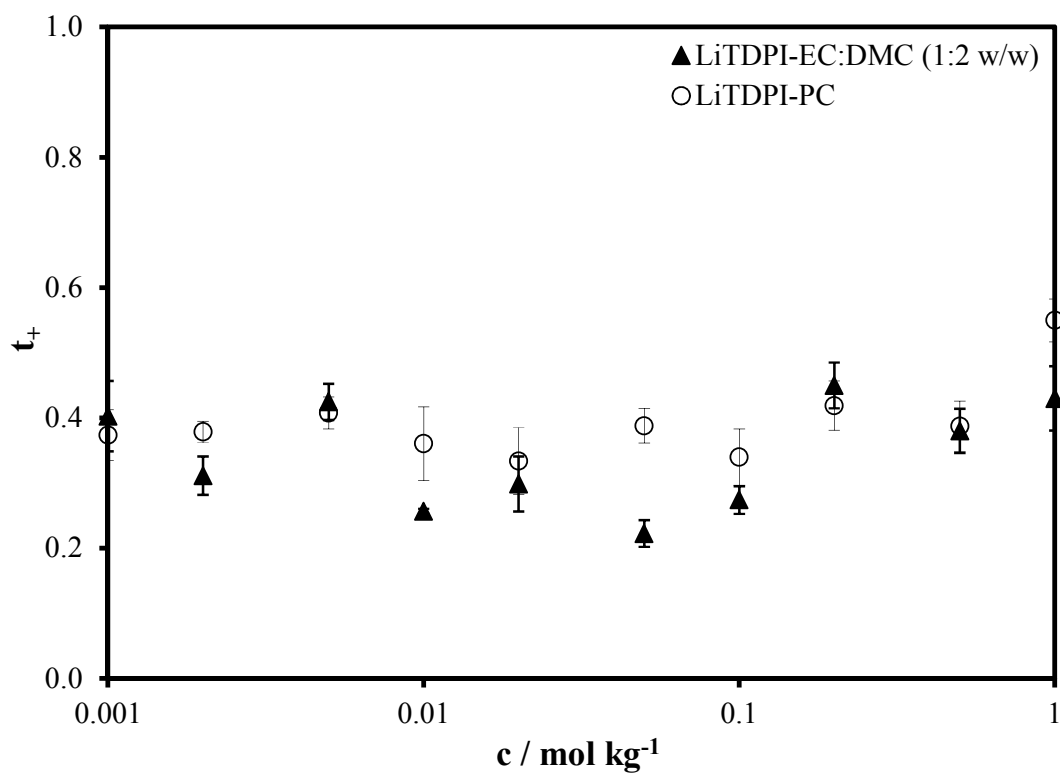


Fig. 7.

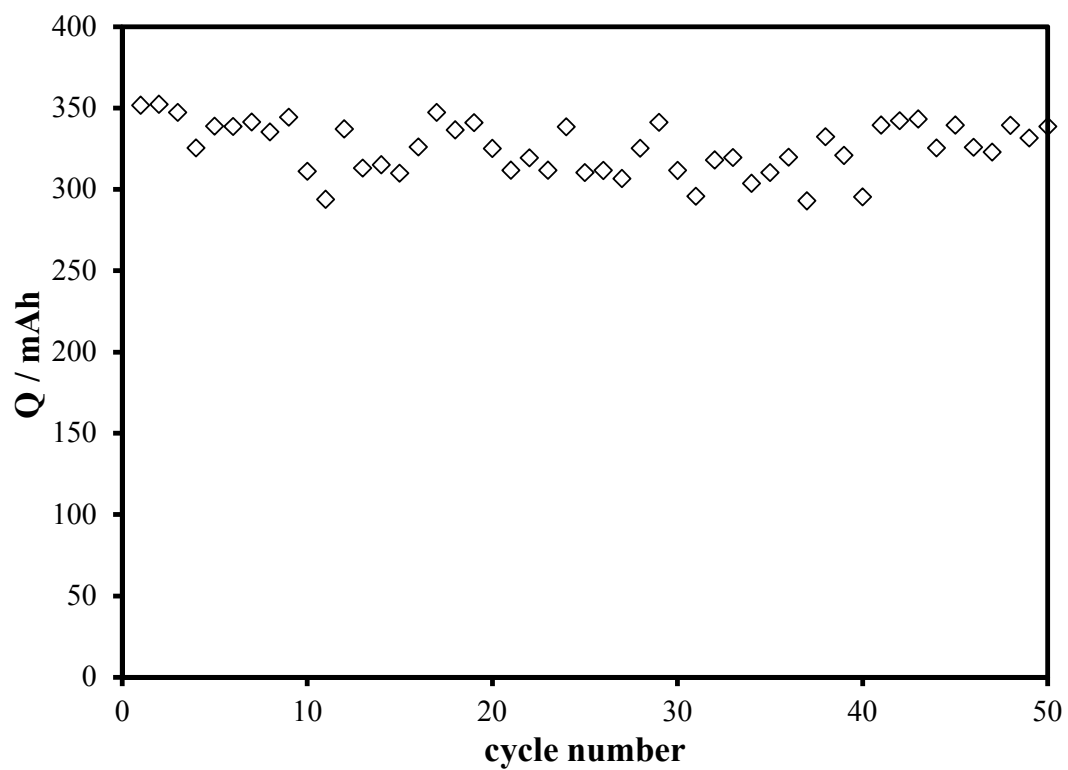


Fig. 8.

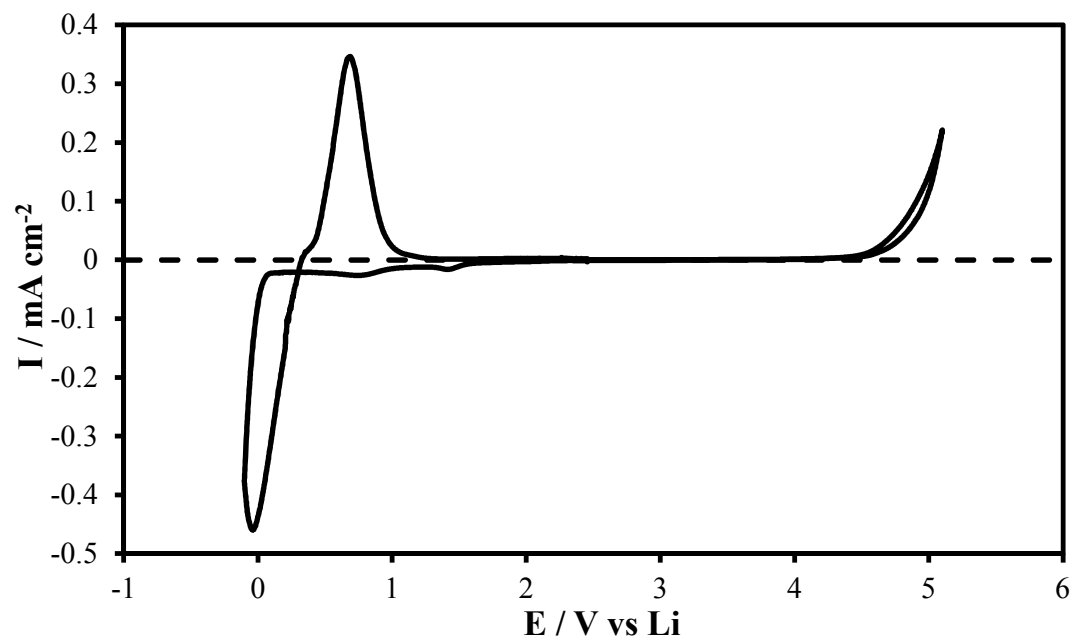


Fig. 9.

